

# Small-Angle Scattering and Electron Microscopy Investigation of Nanotubules Made from a Perfluoroalkylated Glucophospholipid

Toyoko Imae,<sup>\*1</sup> Katsuya Funayama,<sup>\*</sup> Marie Pierre Krafft,<sup>†1</sup> Françoise Giulieri,<sup>‡</sup> Toshio Tada,<sup>§</sup> and Takayoshi Matsumoto<sup>§</sup>

<sup>\*</sup>Department of Chemistry, Faculty of Science, Nagoya University, Nagoya 464, Japan; <sup>†</sup>Chimie des Systemes Associatifs, Institut Charles Sadron, UPR CNRS 22, 6, rue Boussingault, 67083 Strasbourg Cedex, France; <sup>‡</sup>Unité de Chimie Moléculaire, URA CNRS 426, Université de Nice-Sophia Antipolis, Parc Valrose, 06108 Nice Cedex 2, France; and <sup>§</sup>Division of Material Chemistry, Faculty of Engineering, Kyoto University, Kyoto 606, Japan

Received June 26, 1998; accepted January 13, 1999

**Anionic glucophospholipids were recently reported as a new family of tubule-forming lipids. We report here investigations on the structure of nanotubules made from a glucophospholipid with a mixed fluorocarbon–hydrocarbon hydrophobe, using freeze fracture and cryo-transmission electron microscopy (TEM) and X-ray and neutron small angle scattering (SAXS, SANS). The hollow and regularly shaped tubules are very thin: they have an external radius of 140 Å and an internal radius of 35 Å on the average. Their 105 Å-thick wall appears to consist in three bilayers in which the glucophospholipid molecules are probably in a tilted and/or interdigitated configuration. Upon heating these nanotubes convert reversibly into vesicles; transformation is complete at 60°C.**

© 1999 Academic Press

**Key Words:** fluorinated amphiphiles; fluorosurfactants, glucophospholipids; nanotubules; vesicles; nanostructures; self-assembly; small angle neutron scattering; small angle X-ray scattering; transmission electron microscopy.

## INTRODUCTION

Perfluorocarbons and other highly fluorinated compounds have numerous applications including in the medical field where they are being investigated for oxygen delivery (blood substitutes), liquid ventilation, diagnosis, and drug delivery (1–3). Perfluoroalkylated amphiphiles (*F*-amphiphiles) have unique properties including very high surface activities, very low critical micelle concentrations (cmc) (4, 5), and enhanced tendency to self-assemble into supramolecular aggregates (3). Among the *F*-amphiphiles that have recently been synthesized, those with a polar head group of the phosphoglucoside-type are susceptible of being recognized by specific receptors and could therefore be utilized for targeting drugs and other agents to specific tissues (6, 7). Both the alcoholic hydroxyl groups and the acid phosphate group present in phosphoglucosides can be used to bind drugs and facilitate their incorporation into drug delivery systems.

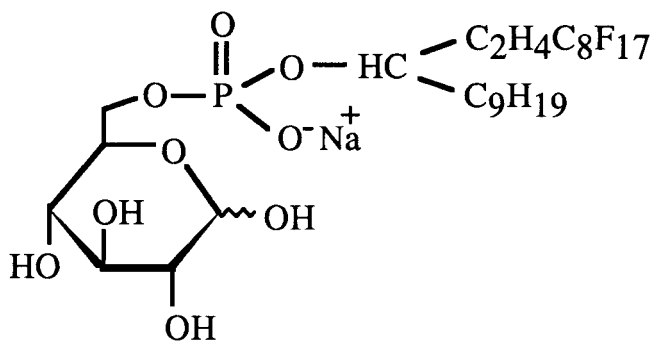
Perfluoroalkylated zwitterionic phosphocholines and phosphatidylcholines, neutral glycolipids and dimorpho-

nophosphates, and anionic glucophospholipids were shown to form vesicles that can be utilized for drug delivery (8–10). These vesicles are significantly more stable than those obtained from hydrogenated analogs. Some *F*-amphiphiles, including dimorpholinophosphates and glucophospholipids, were found to form not only vesicles but also stable hollow bilayer-based micro- and nanotubules (11, 12). The transition from vesicles to such tubules was documented, but no analysis of the structure of the latter assemblies has been carried out yet.

Relatively little information has been published on the structure of tubules and related microstructures made from amphiphilic molecules. Among the few systems rigorously studied by small-angle X-ray scattering (SAXS) and small-angle neutron scattering (SANS) are some gels formed by a steroid derivative in various organic solvents (13–15). These gels were constituted by micron-long rigid fibers (diameter ~100 Å) connected by microcrystalline domains. Results were analyzed on the basis of models of symmetrical double helices (13) and simpler cylindrical rods (14), which both gave satisfactory agreement. Similar analyses were carried out for infinitely long fibers with square or rectangular cross-sections present in organogels of 12-hydroxystearic acid or lithium salt (16, 17) and cholesteryl 4-(2-anthryloxy)butanoate (18). No hollow tubules were reported. Cylindrical fibers were also obtained from *N*-dodecanoyl- $\beta$ -alanine (19, 20). They were more similar to *F*-Glu tubules in the sense that they appear to be constructed by radial multilamellar layers of amphiphiles. They are, however, not hollow.

The number of tubule-forming lipids identified so far is still relatively small and include principally certain alkylaldonamides (21), glutamates (22), glycolipids (23), phospholipid–nucleoside conjugates (24), diacetylenic phospholipids (25), lipid–biotin conjugates (26), porphyrin derivatives (27), and dimorpholinophosphates (28). No investigation using SAXS or SANS has been performed on such tubules, at the exception of those formed from diacetylenic phospholipids. Thomas *et al.* addresses the kinetics of formation of large diacetylenic phosphatidylcholine-based multilamel-

<sup>1</sup> To whom correspondence should be addressed.



**SCHEME 1.** Molecular formula of the fluorinated–hydrogenated glucophospholipid (*F-Glu*) investigated.

lar microtubules (typically of 20  $\mu\text{m}$  in length and 1  $\mu\text{m}$  in diameter) in an ethanol–water mixture (29). X-ray experiments revealed the coexistence of the lamellar chain-melted  $L\alpha$  phase with the chain-frozen  $L\beta$  phase at the temperature of formation of the tubules, indicating that tubule formation is essentially a first-order intralamellar chain-freezing phase transition, i.e., a consequence of passage through the Krafft temperature.

In this work, the formation of nanotubules from an anionic mixed fluorinated–hydrogenated glucophospholipid, and their reversible conversion into small unilamellar vesicles were examined by freeze fracture and cryo-transmission electron microscopy (TEM), SAXS, and SANS. This appears to be the first report of a detailed analysis of tubular structures made from *F*-amphiphiles.

## MATERIALS AND METHODS

Glucophospholipid **1** (*F-Glu*; scheme 1) has a double hydrophobic chain which contains one fluorinated and one hydrogenated branch, grafted through a phosphate linkage to the O-6 position of a glucose polar head group. *F-Glu* was a gift from Prof. J. G. Riess (UCSD, San Diego, CA). Its synthesis was reported in Ref (30). Water was deionized with an Elgastat purification system.  $\text{D}_2\text{O}$  (Aldrich) was used for the TEM and SANS measurements.

### Preparation of Fluorinated Tubules

*F-Glu* (35 mM, 3% w/v) was hydrated for 30 min at 60°C, i.e., above its phase transition temperature (12) and was dispersed in water by sonication for 2 min at 60°C. The pH of the dispersion was measured to be 7. Tubules were formed after 24 h at room temperature and remained stable for at least 3 months.

### Electron Microscopy Experiments

Samples were observed by transmission electron microscopy after freeze fracture (Philips CM12). In the freeze fracture procedure, glycerol (20%) was added to the sample just prior to

freezing. The samples were frozen at  $-110^\circ\text{C}$  in liquid propane and fractured under vacuum using a Balzers cryofract (BAF301,  $2 \times 10^{-6}$  Torr). After Pt/C and rotary carbon depositions, replicas were washed successively with 20% aqueous sodium dodecyl sulfate, ethanol–water (1:1), and distilled water and were eventually picked-up on a 400 mesh grid for examination. Cryo-TEM observations were carried out on a Hitachi H-800 electron microscope using a Hitachi H5001-C cold stage.

### SAXS and SANS Experiments

SAXS was measured by a 6-m point focusing SAXS camera at the High Intensity X-ray Laboratory of Kyoto University. Measurements were carried out at 25°C with an X-ray wavelength of 1.542 Å (CuK $\alpha$  radiation). SANS measurements were performed at room temperature on a WINK small/medium angle diffractometer at the National Laboratory for High Energy Physics (KEK, Tsukuba, Japan); a neutron radiation of 1–16 Å was utilized.

The scattering intensities of very long hollow tubules has been reported by Deutch (31), and can be written as

$$I(Q) = I_0 P(Q)$$

$$P(Q) = (\pi/2QL) \{ [b^2 F(bQ) - a^2 F(aQ)] / (b^2 - a^2) \}^2$$

$$F(x) = 2J_1(x)/x \quad J_1(x) = (\sin x - x \cos x)/x^2 \quad [1]$$

assuming that the interparticle structure factor is unity.  $I_0$  is the scattering intensity at zero scattering angle.  $P(Q)$  is the intraparticle structure factor, and  $a$ ,  $b$ , and  $L$  are, respectively, the internal radius, external radius, and length of the hollow tubule.  $J_1(x)$  is the first-order Bessel function. Intensities were calculated using Eq. [1].

### Volume and Length of the Glucophospholipid's Hydrophobic Chain

The volume of the hydrogenated moiety of the double chain of *F-Glu*,  $v$  ( $\text{\AA}^3$ ), can be calculated from (32)

$$v = 27.4 + 26.9 n_H \quad [2]$$

The volume of the partially fluorinated, partially hydrogenated chain of *F-Glu*,  $v$  ( $\text{\AA}^3$ ), can be calculated from (32, 33):

$$v = 54.5 + 26.9 n_H + 38 n_F \quad [3]$$

where  $n_H$  and  $n_F$  are the numbers of hydrogenated and fluorinated carbons. The volumes occupied by a  $\text{CH}_3$  group and a  $\text{CH}_2$  group are taken as 54.3 and 26.9  $\text{\AA}^3$ , respectively, and those occupied by a  $\text{CF}_3$  group and a  $\text{CF}_2$  group are 92.5 and 38  $\text{\AA}^3$ , respectively (34). The volume of the fluorinated chain,  $\text{C}_8\text{F}_{17}(\text{CH}_2)_2^-$ , was thus found to be 412  $\text{\AA}^3$ , and the volume of

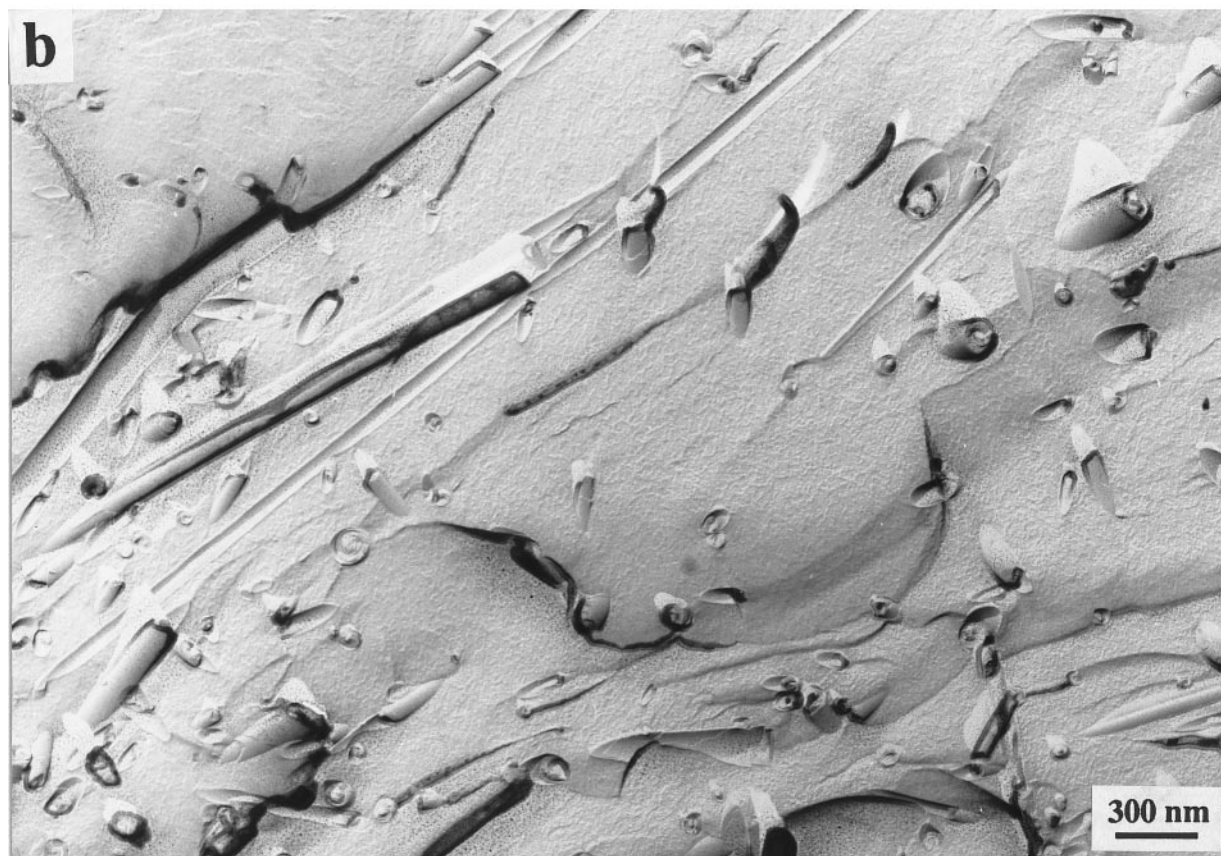
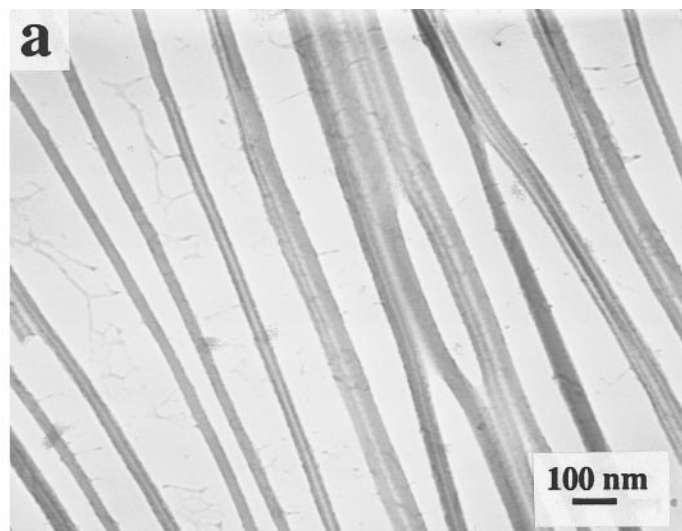


**FIG. 1.** Transmission electron microscopy (TEM) photographs of a 3 w/v% *F*-Glu dispersion at room temperature (ca. 25°C). (a) cryo-TEM; (b) freeze-fracture TEM.

the hydrogenated chain,  $C_9H_{19}-$ , was found to be  $269 \text{ \AA}^3$ . The volume of the *F*-Glu double chain can thus be estimated to be  $681 \text{ \AA}^3$ .

The maximal length of the hydrophobic chain,  $l_c$  ( $\text{\AA}$ ), is obtained from Eq. [4] for hydrogenated amphiphiles (32) and from Eq. [5] for fluorinated amphiphiles (33):

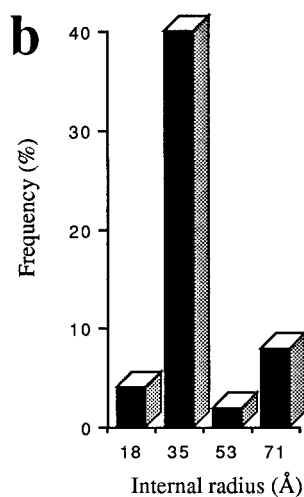
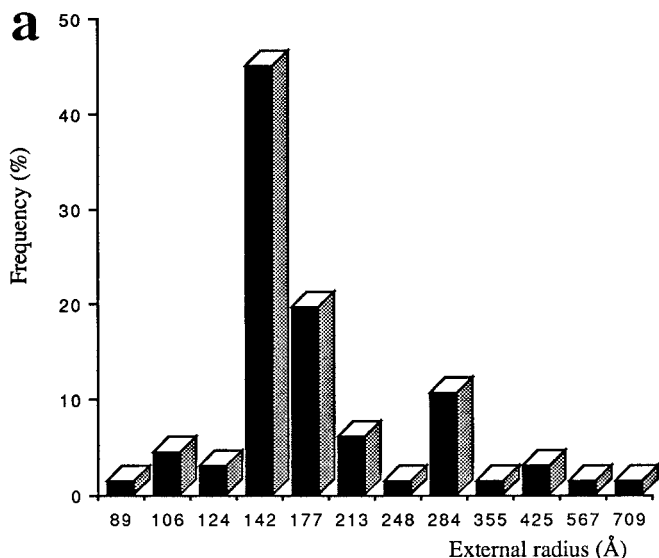


**FIG. 2.** The distribution of cross-sectional radii of *F*-Glu hollow nanotubes. (a) external radius; (b) internal radius.

$$l_c = 1.5 + 1.265 n_H \quad [4]$$

$$l_c = 2.0 + 1.265 n_H + 1.34 n_F \quad [5]$$

The lengths thus calculated are about 15 Å for  $C_8F_{17}(CH_2)_2^-$ , and 13 Å for  $C_9H_{19}^-$ .

## RESULTS

### Structure of the Nanotubes made from the Fluorocarbon-Hydrocarbon Glucophospholipid **1** (*F*-Glu)

At room temperature, the 3% w/v-concentrated dispersion of glucophospholipid **1** (*F*-Glu) has the appearance of a turbid

viscoelastic gel. A cryo-TEM photograph shows that this gel consists in a homogenous population of extremely long and thin tubules with hollow cores (Fig. 1a). The cryo-TEM images allowed determination of the distribution of the external and internal radii of the tubules, as plotted in Fig. 2 (sampling numbers were 66 and 53, respectively). The average external and internal radii of the majority population were found to be about 142 and 36 Å, respectively. The size distribution was rather narrow, especially for the internal radius. A second population (external radius, 280 Å; internal radius, 71 Å) was also observed. The values of radii are double those found for the majority population, indicating that some tubules may have merged to form larger ones. Observation of *F*-Glu tubules by freeze fracture TEM turned out to be difficult because of their strong anisotropy. Figure 1b, however, shows the cross-section of some of the larger tubules present in the sample, evidencing the radial arrangement of the amphiphiles in layers around the aqueous core.

SAXS results for the *F*-Glu dispersion at room temperature are given in Fig. 3a as a double logarithmic plot of scattering intensity  $I(Q)$  vs scattering vector amplitude  $Q$ . The fit between experimental data and calculated values was found to be

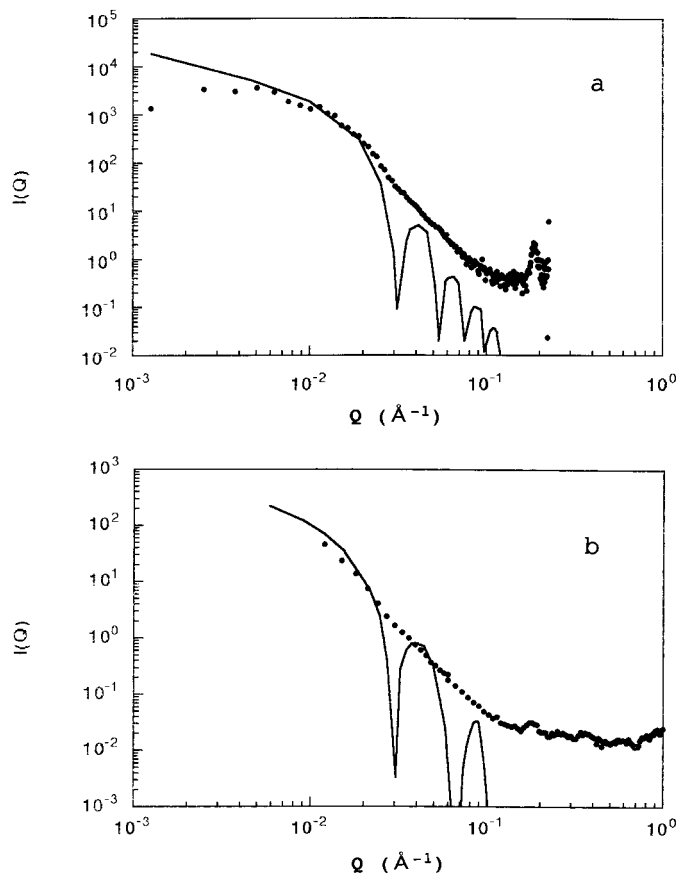


**FIG. 3.** Small-angle scattering of a 3 w/v% *F*-Glu dispersion at room temperature (25°C). (a) SAXS; (b) SANS (●, experimental data; —, theoretical curve).

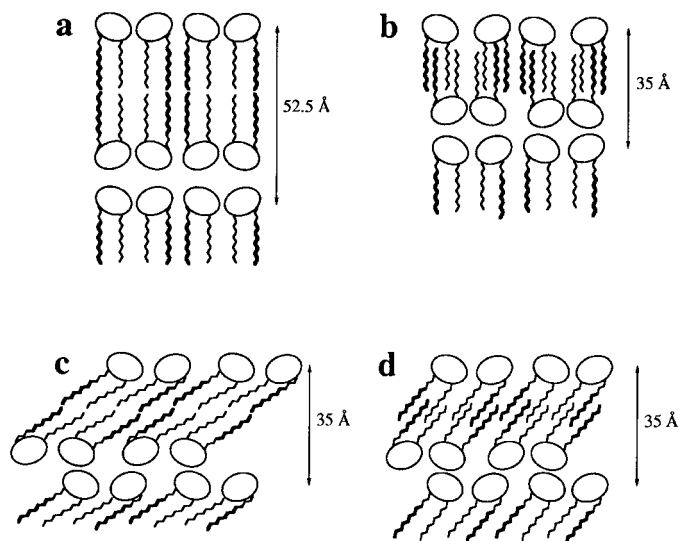


**FIG. 4.** Models for the arrangement of the *F*-Glu molecules in the tubular membrane. (a) regular lamellar arrangement, (b) interdigitated, (c) strongly tilted, (d) partly interdigitated, and tilted. Polar heads are represented slightly tilted in order to compensate for the difference in length between the fluorinated and the hydrogenated chain.

optimum for an external radius,  $b$ , of 140 Å and an internal radius,  $a$ , of 35 Å. These values are in good agreement with those obtained by cryo-TEM images. The discrepancies between the theoretical curve and experimental data can originate from different sources. The polydispersity in external radius explains the absence of minima of the experimental curve as compared to the theoretical oscillation curve (coming from the Bessel function). It can also be seen that the experimental curve does not fit with the maxima of the theoretical oscillations; this comes from the fact that a simple model based on a hollow tube without any concentric layers was taken for the calculation. Improving this model is the subject of future investigations to obtain detailed information on these tubules. The discrepancy seen at high  $Q$  values is probably due to the polydispersity of the external radius (13). The discrepancy seen at low  $Q$  values originates from the interactions between tubules (see Fig. 1a) and is due to the contribution of the interparticle structure factor (35) which was neglected in the calculation. A comparable scattering profile was obtained by SANS at 25°C (Fig. 3b).

From the values of the geometric parameters ( $b = 140$  Å;  $a = 35$  Å), one can deduce that the thickness of the shell of the hollow tubules in their cross-section is 105 Å. Using Tanford's equations (32), one can calculate the length of the fluorinated chain  $C_8F_{17}(CH_2)_2 - (15$  Å) (33), and that of the hydrogenated chain  $C_9H_{19} - (13$  Å). This allows us to evaluate the length of the hydrophobic part of *F*-Glu to be about 15 Å. The literature indicates that the surface of a glucose polar head group is ca 75 Å<sup>2</sup> (36), a value which is comparable to that found for hydrated phospholipids (37). The molecular length of the *F*-Glu molecule can thus be reasonably estimated to be about 25 Å.

Assuming from freeze fracture TEM images that the *F*-Glu molecules display a layer arrangement in the radial direction of the shell, we can therefore propose that the 105 Å-thick shell of the tubules is composed either of two bilayers having a thickness of 52.5 Å each, which corresponds to twice the molecular length, or of three bilayers having a thickness of 35 Å. Four different models can thus be proposed for the arrangement of the *F*-Glu molecules in the tubular membrane, as illustrated in Fig. 4. The first one consists in a regular bilayer arrangement of the molecules (a). In the other ones, the amphiphiles are interdigitated (b), strongly tilted (c), or both tilted (with a smaller tilt angle than in (b), however) and partially interdigitated (d). In each case distances include the water shell.

As seen in the SAXS pattern of Fig. 5, a Bragg peak was obtained at  $Q_{\text{peak}} = 0.185$  Å<sup>-1</sup>. A weak Bragg peak was also observed by SANS for the same  $Q$  value. Since the shell of the hollow tubule has a layered arrangement, the Bragg peak at 0.185 Å<sup>-1</sup> may be assigned to be a (001) reflection in the lamellar unit cell structure. The repeating distance of the lamellar array is then 34 Å ( $= 2\pi/Q_{\text{peak}}$ ). This value is in good agreement with models (b), (c), and (d) of interdigitated and/or tilted bilayers. On the other hand, it makes model (a) rather unlikely.

#### Tubule-to-Vesicle Transition in the *F*-Glu Dispersion

Dispersions of *F*-Glu were incubated at various temperatures and observed by freeze fracture and cryo-TEM, as illustrated in Fig. 6. At 40°C, tubules were still present but their morphology was slightly modified (Fig. 6a). Some tubules retained their original shape, while others seemed to have merged. Their aqueous core was no more systematically visible. When the temperature was raised to 50–60°C, vesicles of various sizes started to appear and coexisted with tubules, as well as pre-

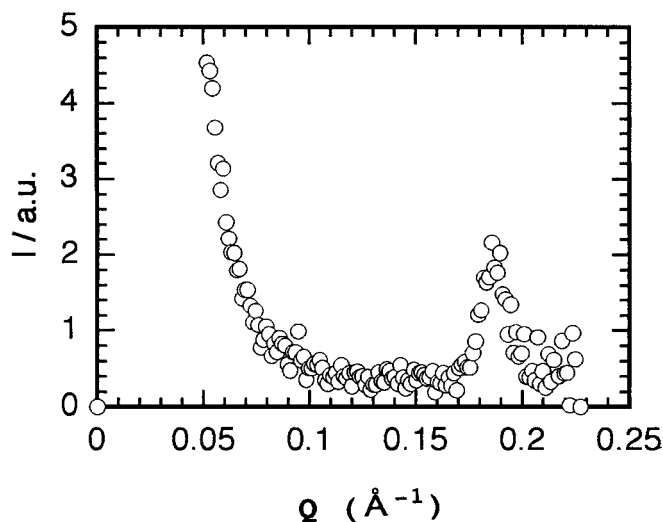


**FIG. 5.** Small angle X-ray scattering of a 3% w/v *F*-Glu dispersion at room temperature (25°C).

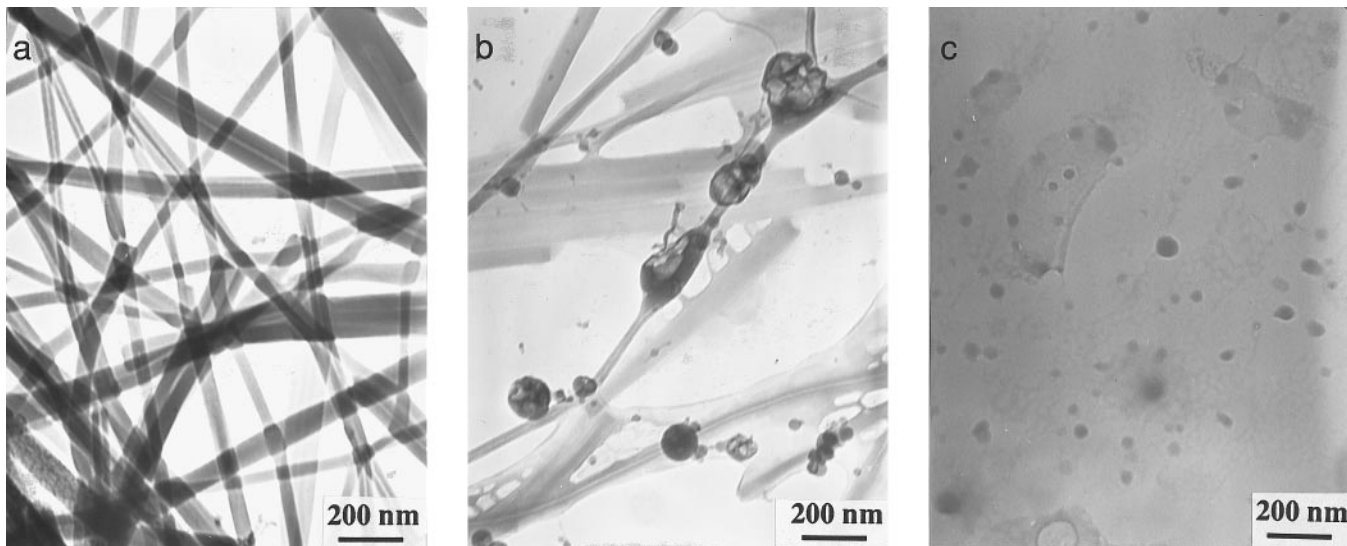


**FIG. 6.** Cryo-TEM photographs of a 3% w/v *F*-Glu dispersion showing the transformation between (a) nanotubes (at 40°C) and (c) vesicles (at 60–70°C). (b) The intermediate structures that are formed during the conversion (50–60°C).

curved vesicles in their process of formation (Fig. 6b). Various types of transition processes occur, as schematically illustrated in Fig. 7. For example, some vesicles seemed to

protrude from swollen bilayers expanding from tubules. Others appeared to form from tubules that were clutched, then cut at various levels of their length. At 60–70°C, only vesicles were seen (Fig. 6c).

SAXS intensity was measured at 60°C (Fig. 8). Unfortunately, the Bragg peak intensity was too low to allow a determination of the  $Q_{\text{peak}}$  value and to calculate the repeating distance in the membrane of *F*-Glu vesicles. Since the presence of these vesicles, as evidenced by freeze fracture and cryo-TEM, is not questionable, it can be hypothesized that the vesicle's multilayer membrane is less well-organized than that of the tubules or that only unilamellar vesicles are present.

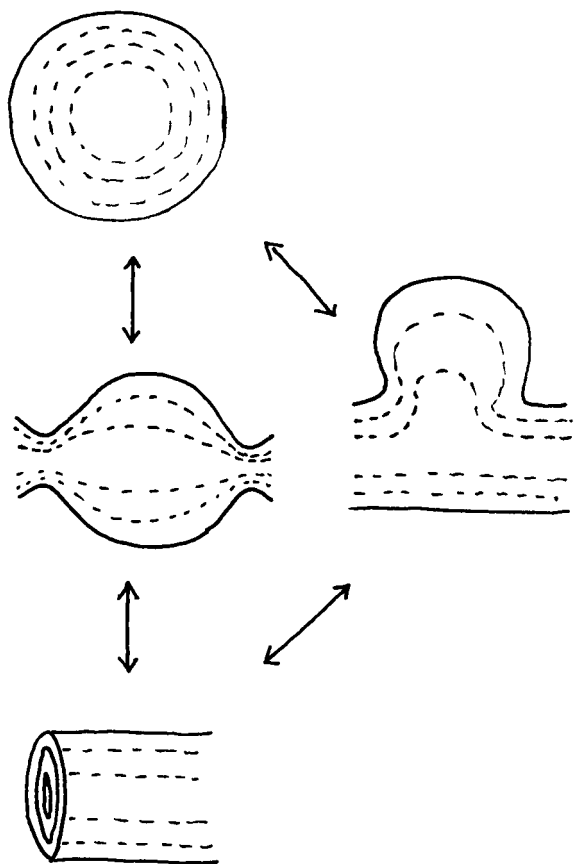


**FIG. 7.** Schematic illustration of various types of transition processes between *F*-Glu vesicles and hollow tubules.

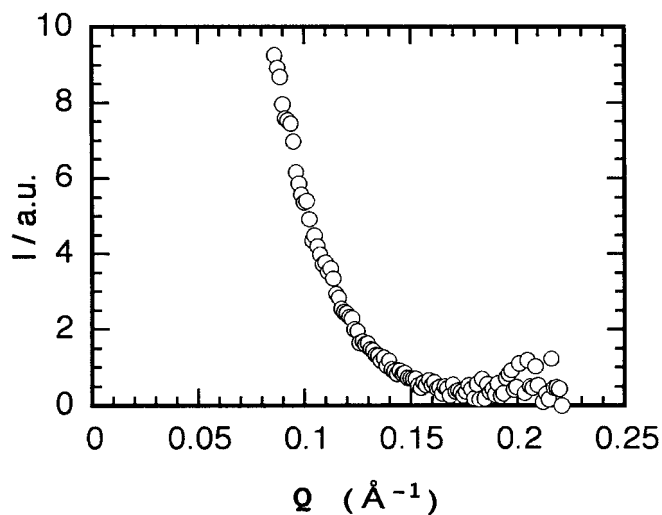


**FIG. 8.** Small angle X-ray scattering of a 3 w/v% *F*-Glu dispersion at 60°C.

## DISCUSSION

The above experiments allowed us to characterize nanotubules made from fluorinated glucophospholipids (*F*-Glu) and determine their internal and external radii and the number of rolled-up bilayers of the lipidic walls. These experiments also allowed us to eliminate the model of a regular lamellar arrangement of *F*-Glu molecules. Although no experimental data are available that will help to decide in favor of model (b), (c), or (d), some comments can be made. Figure 9a shows the cross-sections of the polar head (estimated to be  $\sim 75 \text{ \AA}^2$ ), fluorinated chain ( $30 \text{ \AA}^2$ ), and hydrogenated chain ( $20 \text{ \AA}^2$ ) in the *F*-Glu molecule. Figure 9b shows what happens when a fluorinated chain and a hydrogenated chain are added, as a consequence of chain interdigitation. In order to assess the steric hindrance resulting from chain interdigitation, we have calculated the *F*-Glu's "packing parameter,"  $P = v/a_0l_c$  ( $v$  is the hydrophobic chain's volume,  $a_0$  is the polar head surface area at the cmc, and  $l_c$  is the chain length) (38), in the presence and absence of interdigitation. Israelachvili's concept of "optimal surface area" per polar head, which corresponds to the minimal total free energy per amphiphile molecule, allows the prediction of the formation and type of aggregates. If  $P < \frac{1}{3}$ , the amphiphile is expected to form spherical micelles; if  $\frac{1}{3} < P < \frac{1}{2}$ , rod-like micelles will tend to form; if  $\frac{1}{2} < P < 1$  bilayers with a spontaneous curvature (vesicles) will be observed; if  $P = 1$ , planar bilayers will form; and if  $P > 1$ , aggregates with a reverse curvature will form. In the absence of interdigitation the calculated  $P$  value ( $P = 0.6$ ) indicates that *F*-Glu tends to form bilayers which can evolve to vesicles. This result is supported by our experimental observation: *F*-Glu tubules do convert into vesicles upon heating. The formation of tubules, however, is not taken in consideration by the model. By contrast, the  $P$  value is 1.2 in the interdigitated configuration. This value would suggest the formation of aggregates with a reverse curvature, which was not observed experimen-

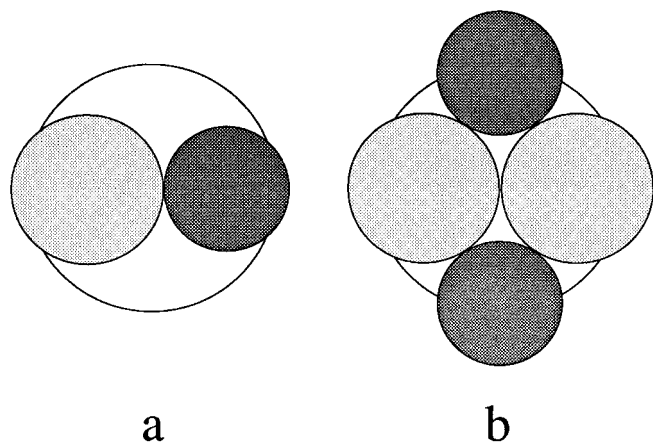


FIG. 9. Cross-sectional view of the *F*-Glu molecule (a) noninterdigitated conformation; (b) interdigitated conformation.

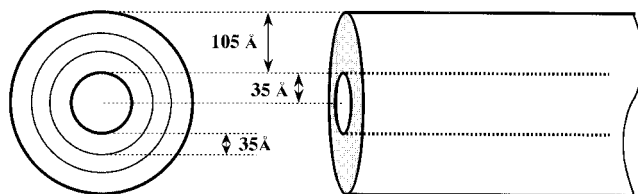


FIG. 10. Schematic representation of nanotubules of *F*-Glu. The 105 Å-thick walls are constructed by three bilayers of *F*-Glu molecules.

tally. As a consequence, model (b), in which chains are totally interdigitated appears rather unlikely. However, if one keeps in mind the mixed character, partially fluorinated, partially hydrogenated, of the *F*-Glu molecule, we can expect that interdigitation may be favored, at least to some extent. The confinement resulting from the chemical grafting onto the polar head of such antinomic hydrophobes, the fluorinated chain and the hydrogenated one, may indeed induce their mutual repulsion. The mixing of fluorocarbons and hydrocarbons is highly nonideal (39). This results from the difference in cohesive energy between the two types of molecules. As a consequence, it was shown that fluorinated and hydrogenated amphiphiles show only limited miscibility when present simultaneously in liposomes (40). The repulsion between the fluorinated and the hydrogenated chain may increase the degree of freedom and consequently the degree of hydration of the glucose polar head, which in turn may facilitate interdigitation. As a consequence, one can consider that model (d), in which the molecules are partly interdigitated and tilted, to be acceptable. In model (c), the amphiphiles are not interdigitated at all; as a consequence, they have to be strongly tilted in order to form a 35 Å-thick bilayer. Up to now, we do not have any means to choose between models (d) and (c).

As a conclusion, our experiments showed that the nanotubules made from the fluorinated glucophospholipid *F*-Glu have external and internal radii of about 140 and 35 Å, respectively, as illustrated in Fig. 10. Their 105 Å-thick lipidic walls are constructed by three interdigitated and/or tilted bilayers. It must be emphasized that such thin tubules are quite different from the other ones reported in the literature. Much thinner than those obtained from diacetylenic phospholipids (typical diameter:  $\sim 1 \mu\text{m}$ ) (25), they are closer to those formed by *N*-octyl-D-galactonamide (typical diameter: 50–100 nm) (21). Investigations on the totally hydrogenated analog of *F*-Glu that forms large multilayered microtubules (microns in diameter) very comparable to that of diacetylenic phospholipids and that convert into large vesicles are presently underway, in order to evaluate the impact of the fluorinated chain on the curvature of the tubular membrane.

## ACKNOWLEDGMENTS

The authors thank Prof. J. G. Riess for samples of the glucophospholipid as well as for advice and useful discussions. They are grateful to Prof. M.

Furusaka and Dr. S. Shimizu of KEK (Tsukuba, Japan) for their permission and assistance in SANS measurements and to Mr. T. Iwamoto of Nagoya University for his help in TEM measurement. They also thank the Japanese Society for the Promotion of Science (JSPS) and the Centre National de la Recherche Scientifique (CNRS) for support.

## REFERENCES

1. Riess, J. G., *Colloids Surf.* **84**, 33 (1994).
2. Krafft, M. P., and Riess, J. G., *Biochimie* **80**, 489 (1998).
3. Riess, J. G., and Krafft, M. P., *Biomaterials* **19**, 1529 (1998).
4. Kissa, E., "Fluorinated Surfactants. Synthesis, Properties, Applications." p. 469. Marcel Dekker, New York, 1994.
5. Greiner, J., Riess, J. G., and Vierling, P., in "Organofluorine Compounds in Medicinal Chemistry and Biomedical Applications" (R. Filler, Y. Kobayashi and L. M. Yagupolski, Eds), p. 339. Elsevier, Amsterdam, 1993.
6. Jones, M. N., *Adv. Drug Delivery Rev.* **13**, 215 (1994).
7. Guillot, F., Greiner, J., and Riess, J. G., *Biochim. Biophys. Acta* **1282**, 283 (1996).
8. Krafft, M. P., Giulieri, F., and Riess, J. G., *Angew. Chem. Int. Ed. Engl.* **32**, 741 (1993).
9. Riess, J. G., *J. Drug Targeting* **2**, 455 (1994).
10. Riess, J. G., Frézar, F., Greiner, J., Krafft, M. P., Santaella, C., Vierling, P., and Zarif, L., in "Handbook of Nonmedical Applications of Liposomes" (Y. Barenholz and D. D. Lasic, Eds.), Vol. III, p. 97. CRC Press, Boca Raton, 1996.
11. Giulieri, F., Krafft, M. P., and Riess, J. G., *Angew. Chem. Int. Ed. Engl.* **34**, 1514 (1996).
12. Giulieri, F., Guillod, F., Greiner, J., Krafft, M. P., and Riess, J. G., *Chem. Eur. J.* **2**, 1335 (1996); Imae, T., Krafft, M. P., Giulieri, F., Matsumoto, T., and Tada, T., *Progr. Colloid Polym. Sci.* **106**, 52 (1997).
13. Terech, P., Volino, F., and Ramasseul, R., *J. Phys.* **46**, 895 (1985).
14. Terech, P., *Progr. Colloid Polym. Sci.* **82**, 263 (1990).
15. Wade, H. R., Terech, P., Hewat, E. A., Ramasseul, R., and Volino, F., *J. Colloid Interface Sci.* **114**, 442 (1986).
16. Terech, P., *J. Phys. II France* **2**, 2181 (1992).
17. Terech, P., Rodriguez, V., Barnes, J. D., and McKenna, J. B., *Langmuir* **10**, 3406 (1994).
18. Terech, P., Furman, I., and Weiss, R. G., *J. Phys. Chem.* **99**, 9558 (1995).
19. Imae, T., Takahashi, Y., and Muramatsu, H., *J. Am. Chem. Soc.* **114**, 3414 (1992).
20. Imae, T., Hayashi, N., Matsumoto, T., and Furusaka, M., in preparation.
21. Fuhrhop, J. H., and Helfrich, W., *Chem. Rev.* **93**, 1565 (1993).
22. Nakashima, N., Asakuma, S., and Kunitake, T., *J. Am. Chem. Soc.* **107**, 509 (1985).
23. Zarif, L., Gulik-Krywicki, T., Riess, J. G., Pucci, B., Guedj, C., and Pavia, A. A., *Colloids Surf.* **84**, 107 (1993).
24. Yanagawa, H., Ogawa, Y., Futura, H., and Tsuno, K., *J. Am. Chem. Soc.* **111**, 4567 (1989).
25. J. Schnur, *Science* **262**, 1669 (1993).
26. Ringler, P., Müller, W., Ringsdorf, H., and Brisson, A., *Chem. Eur. J.* **3**, 620 (1997).
27. Fuhrhop, J. H., Bindig, U., and Siggel, U., *J. Am. Chem. Soc.* **115**, 11036 (1993).
28. Krafft, M. P. and Giulieri, F., in preparation.
29. Thomas, B. N., Safinya, C. R., Plano, R. J., and Clark, H. A., *Science* **267**, 1635 (1995).
30. Guillod, F., Greiner, J., and Riess, J. G., *Carbohydr. Res.* **261**, 37 (1994).
31. Deutch, J. M., *Macromolecules* **14**, 1826 (1981).
32. Tanford, C., "The Hydrophobic Effect." Wiley, New York, 1980.
33. Giulieri, F., and Krafft, M. P., *Colloids Surf.* **84**, 121 (1994).
34. Tiddy, G. J. T., in "Modern Trends of Colloid Science in Chemistry and Biology." (H. F. Eicke, Eds.), p. 148. Birkhauser, Basel, 1985.
35. Kakitani, M., Imae, T., and Furusaka, M., *J. Phys. Chem.* **99**, 16018 (1995).
36. Shipley, G. G., Green, J. P., and Nichols, B. W., *Biochim. Biophys. Acta* **311**, 531 (1973).
37. Cevc, G., "Phospholipids Handbook." Marcel Dekker, New York, 1993.
38. Israelachvili, J., Mitchell, D. J., and Ninham, B. W., *J. Chem. Soc., Faraday Trans.* **2**, 72 (1976) 1525.
39. Hildebrandt, J. H., Prausnitz, J. M., and Scott, R. L. "Regular and Related Solutions" Van Nostrand Reinhold, New York, 1970.
40. Elbert, R., Folda, T., and Ringsdorf, H., *J. Am. Chem. Soc.* **106**, 7687 (1984).